Resonances in photodetachment of $H^-(2p^2\,{}^3P^e)$

Jian-Zhi Tang,[1] C. D. Lin,[2] Bin Zhou,[2] and Isao Shimamura[1]
[1] *The Institute of Physical and Chemical Research (RIKEN), Hirosawa 2-1, Wako-shi, Saitama 351-01, Japan*
[2] *Department of Physics, Kansas State University, Manhattan, Kansas 66506-2601*
(Received 31 August 1994)

The cross sections for the photodetachment from the second bound state of the negative hydrogen ion, $H^-(2p^2\,{}^3P^e)$, for photon energies above the $H(n=2)$ threshold are calculated using a hyperspherical close-coupling method. This state is parity forbidden to autoionize into $H(n=1)+e$ and has an extremely small binding energy of 0.01 eV. The results for low photon energies agree with earlier calculations. For energies near the $H(n=3)$ threshold, two shape resonances are found in addition to many Feshbach resonances. These resonances are identified by examining adiabatic hyperspherical potential-energy curves.

PACS number(s): 32.80.Fb, 32.80.Dz, 31.50.+w

I. INTRODUCTION

In an earlier paper [1], the photodetachment cross sections of H^- from the ground state were examined using a hyperspherical close-coupling (HSCC) method for energies up to the threshold for the production of $H(N=4)$, where N is the principal quantum number. The calculated photodetachment cross sections were in good agreement with experimental data [2]. The HSCC calculations were recently extended up to the $H(N=7)$ threshold [3] and good agreement with experiment [4] was found again. The HSCC method was also applied to calculate photoabsorption cross sections of helium [5–7] and other two-electron systems [8] from the ground state and of helium from excited states [9–11].

In the present work, we studied the photodetachment of H^- from the second bound state, namely, the $H^-(2p^2\,{}^3P^e)$ state. The energy of this state lies in the continuum $H(1s)+\epsilon p$, but its autoionization is parity forbidden. We do not anticipate that such photodetachment experiments may be carried out in the near future, but the calculations were performed for the following reasons.

(1) To locate and identify many shape and Feshbach resonances of H^- associated with high-N thresholds. Many of these resonances were calculated and identified recently, for example, by Ho and Bhatia [12,13] using a complex-coordinate rotation method with variational wave functions.

(2) To study the effect of the extremely weak binding of $H^-(2p^2\,{}^3P^e)$, or of its diffuse wave function, on the photodetachment cross sections and their resonance structures. The binding energy with respect to the $H(N=2)$ threshold is 0.01 eV, which is much smaller than the binding energy 0.75 eV of the ground state $H^-(1s^2\,{}^1S)$.

(3) To compare the photodetachment cross sections with those calculated by Jacobs *et al.* [14] using three-state close-coupling wave functions for the final continuum states, and with the recent results of Du *et al.* [15] and Starace [16], who calculated the cross sections at low energies using a semiempirical adiabatic hyperspherical approximation.

Details of the theoretical method were described elsewhere [5,9]; only the essentials are mentioned briefly in Sec. II in this paper. The results are presented in Sec. III with some discussion, and a conclusion is given in Sec. IV. Atomic units are used throughout unless otherwise noted.

II. HYPERSPHERICAL CLOSE-COUPLING METHOD

In the hyperspherical coordinates, the two-electron wave function of H^- is expressed as $\Psi(\mathbf{r}_1,\mathbf{r}_2) = (R^{5/2}\sin\alpha\cos\alpha)^{-1}\Phi(R,\alpha,\Omega)$, where $R=(r_1^2+r_2^2)^{1/2}$ is the hyperradius, $\alpha=\arctan(r_2/r_1)$ is the hyperangle, and Ω denotes collectively the four angles $(\hat{\mathbf{r}}_1,\hat{\mathbf{r}}_2)$. To solve the Schrödinger equation, the configuration space is divided into two regions: the inner one ($R<R_M$) where the electron-electron interaction is strong and the outer or asymptotic region ($R>R_M$) where the electron-electron interaction is relatively weak and electron exchange is negligible. In the inner region, the wave function $\Phi_\beta^{(\mathrm{in})}$, which is the βth independent solution of the inner-region Schrödinger equation, is expressed in a close-coupling expansion

$$\Phi_\beta^{(\mathrm{in})}(R,\alpha,\Omega)=\sum_{\mu=1}^{N_{\mathrm{ch}}} F_\mu(R)\phi_\mu(\alpha,\Omega;R), \tag{1}$$

where N_{ch} is the number of channels included. The diabatic basis functions ϕ_μ are defined in detail in Ref. [5]. Substituting Eq. (1) into the Schrödinger equation, one obtains close-coupling equations for $F_\mu(R)$.

Beyond $R=R_M$, the two electrons are well separated, i.e., one is relatively close to the nucleus and the other is far away, and the outer-region wave function $\Psi_\beta^{(\mathrm{out})}(\mathbf{r}_1,\mathbf{r}_2)$ is expanded in terms of the hydrogen wave functions. This expansion leads to the usual independent-electron close-coupling equations. They may be decoupled, by a unitary channel transformation, within a block of channels associated with degenerate excited states N [17–19], if we neglect potentials of a range shorter than the dipole potential throughout the outer region. We choose R_M to be so large that this is a good approximation.

The solutions of each uncoupled equation are of the Bessel class and are well known [17,18,20]. For open channels, we may define two linearly independent energy-normalized solutions $s_j(k_n r_2)$ and $c_j(k_n r_2)$ that behave asymptotically like sine and cosine functions, where $\frac{1}{2}k_n^2 = \epsilon_n$ is the channel energy, or the total energy E plus the binding energy $1/2n^2$ of the hydrogen atom. For closed channels, we may find a solution $f_j(r_2)$ that decays exponentially with r_2. The wave function in the outer region is then expressed as

$$\Psi_\beta^{(\mathrm{out})} = r_2^{-1} \sum_{j,\mathrm{open}} \varphi_j(\mathbf{r}_1, \hat{\mathbf{r}}_2)[s_j(k_n r_2) I_{j\beta} - c_j(k_n r_2) J_{j\beta}] + r_2^{-1} \sum_{j,\mathrm{closed}} \varphi_j(\mathbf{r}_1, \hat{\mathbf{r}}_2) f_j(r_2) C_{j\beta} \quad (R \geq R_M), \tag{2}$$

where $\varphi_j(\mathbf{r}_1, \hat{\mathbf{r}}_2)$ is a channel function obtained by diagonalizing the asymptotic Hamiltonian, and is a linear combination of products of hydrogenic wave functions and the angular wave functions of the other electron.

By performing two-dimensional matching of the two functions $\Psi_\beta^{(\mathrm{out})}$ and $\Psi_\beta^{(\mathrm{in})} = (R^{5/2}\sin\alpha\cos\alpha)^{-1}\Phi_\beta^{(\mathrm{in})}$ on the hyperspherical surface $R = R_M$, the coefficients $I_{j\beta}$, $J_{j\beta}$, and $C_{j\beta}$ are determined, from which the reaction matrix K is calculated.

This procedure was carried out for the final continuum states as well as for the initial $H^-(2p^2\,^3P^e)$ bound state. We chose $N_{\mathrm{ch}} = 36$ and $R_M = 400$ for the former. For the latter, we chose $N_{\mathrm{ch}} = 24$ and $R_M = 380$. This choice of the matching radius, which is quite large for a bound state, was necessary because of the extremely diffuse wave function, as explained in Sec. I, item (2). The total binding energy was calculated to be $-0.125\,351$ in good agreement with a result $-0.125\,350$ of an elaborate variational calculation [21]. This necessitates no artificial adjustment of potential-energy curves to reproduce the correct binding energy, such as was made empirically in Ref. [15].

Once the initial- and final-state wave functions are calculated, the dipole matrix elements and the photodetachment cross sections may be calculated. We used both the length and the acceleration forms of the dipole transition operator. The two different forms led to results in agreement with each other within two significant figures at most energies. However, the convergence of the acceleration-form cross section with N_{ch} was found to be extremely slow close to the $N = 2$ threshold. This was shown elsewhere [22] to be due to the significant cancellation among contributions to a dipole-acceleration matrix elements from various different channels μ. Therefore, only the results of length-form calculations are presented in this paper.

III. RESULTS AND DISCUSSION

We first present in Fig. 1 the global partial cross sections for photodetachment in which the hydrogen atom is left in the $2s$ or $2p$ excited state. Both partial cross sections drop rapidly with increasing energy after a sharp peak near the $H(N = 2)$ excitation threshold. Also presented in the figure are the results by Jacobs *et al.* [14], which are discussed below. Numerous resonances appear in each channel as the photon energy approaches each excitation threshold. In the following, the calculated results are analyzed.

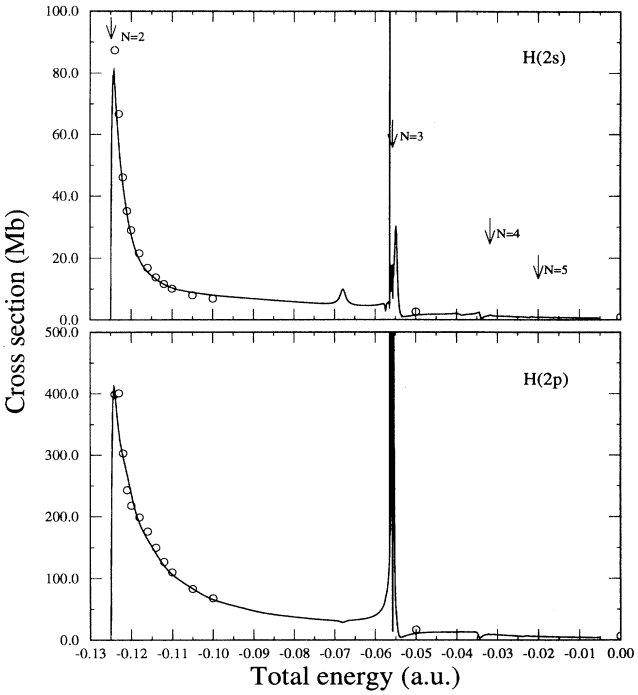

FIG. 1. Partial cross sections for photodetachment from the $H^-(2p^2\,^3P^e)$ state to final states with the H atom left in (a) the $2s$ state, or (b) the $2p$ state. The solid curves represent the present results, and the circles the results of Jacobs *et al.* [14]. The downward arrows indicate the thresholds for the production of $H(N)$.

A. Cross sections near the H($N = 2$) threshold

The photodetachment cross sections in the low-energy region were calculated by Jacobs *et al.* [14] using $1s$-$2s$-$2p$ three-state close-coupling wave functions for the final state and an 84-term Hylleraas-type wave function for the initial state. Their results are shown by circles in Fig. 1 and are in good agreement with the present results except that their calculations were terminated before the present cross sections drop sharply toward the $H(N = 2)$ threshold. Since the initial state is $^3P^e$, the final states populated are $^3P^o$ and $^3D^o$ states. The open channels below the $H(N = 3)$ threshold are

$$\begin{aligned} h\nu + H^-(2p^2\,^3P^e) &\rightarrow H(1s) + \epsilon p(^3P^o) \\ &\rightarrow H(2s) + \epsilon p(^3P^o) \\ &\rightarrow H(2p) + \epsilon s(^3P^o) \\ &\rightarrow H(2p) + \epsilon d(^3P^o) \\ &\rightarrow H(2p) + \epsilon d(^3D^o). \end{aligned} \tag{3}$$

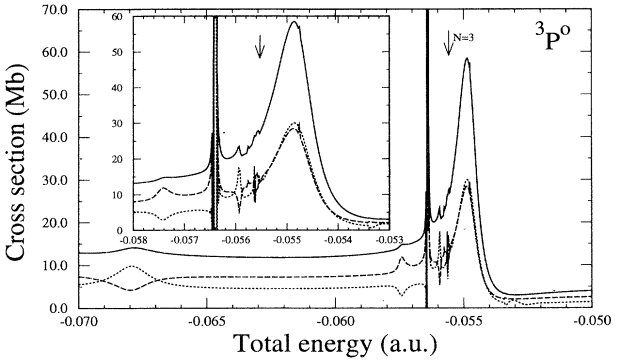

FIG. 2. Cross sections for photodetachment from the $H^-(2p^2\,^3P^e)$ state to final states $H(N=2)+\epsilon l$ $(^3P^o)$ in the energy region near the $H(N=3)$ threshold indicated by the arrow. Dotted curves: H(2s) partial cross section. Dashed curves: H(2p) partial cross section. Solid curves: sum of these cross sections. The inset is a magnification of a region close to the $H(N=3)$ threshold.

Thus three continuum channels of $^3P^o$ symmetry are degenerate, which introduces an effective dipole potential as explained in Sec. II, and the H(2s) and H(2p) partial cross sections are theoretically finite at the threshold $H(N=2)$ [17,18,23], although the calculated results in Fig. 1 might look as if they approached zero.

The rapid drop of these cross sections near the threshold was found also in the recent calculations of Du *et al.* using hyperspherical coordinates within the adiabatic approximation [15]. Their results for the 2p partial cross section and for the sum of the 2p and 2s partial cross sections are close to our results and those of Jacobs *et al.* [14]. However, the smaller 2s partial cross section obtained by Du *et al.* [15] and Starace [16] differed from ours and from the results of Jacobs *et al.* and was not presented here. Reference [15] also discussed the importance of the couplings among the adiabatic hyperspherical channels, which were neglected in their calculations.

B. $^3P^o$ resonances near the $H(N=3)$ threshold

The contributions to the 2s and 2p partial cross sections and to their sum from $^3P^o$ final continuum states near the $N=3$ threshold are shown in Fig. 2. Five Feshbach resonances in the spectra were identified and their positions and widths were calculated by fitting the spectra to the Fano-profile formula [24]. The results are listed in Table I and are compared with those calculated variationally by Ho and Bhatia [12,13] using Hylleraas- or Slater-type basis functions and the complex-coordinate rotation method. Table I also compares the results with those obtained by Pathak *et al.* [19] using the *R*-matrix method. We note that all these calculations agree well with each other.

It is interesting to note that the first resonance has almost a Lorentzian shape for the 2s partial cross section, but is a window resonance for the 2p partial cross section. It is just the opposite for the second resonance. In fact, the two partial cross sections add up to a nearly flat curve such that there is only a slight indication of resonances in the total cross section for the production of $H(N=2)$ in this energy region. Three other sharp resonances are clearly seen in all the three cross sections below the $N=3$ threshold which is marked by a downward arrow.

Figure 2 also shows a pronounced shape resonance in the $^3P^o$ channel above the $N=3$ threshold, which dominates the $^3P^o$ photodetachment cross section in this energy region. The fitted position and width of this shape resonance are included in Table I together with the results of Refs. [12] and [19]. Our results agree well with those of Ho and Bhatia [12] but differ substantially from those of Pathak *et al.* [19], especially in the width.

To identify the resonances calculated above, it is useful to examine the adiabatic hyperspherical potential curves. The $^3P^o$ curves near the $N=3$ threshold are shown in Fig. 3. There are five adiabatic channels converging to the $N=3$ threshold. In the asymptotic region, as detailed more clearly in the inset, three potential curves approach the $N=3$ threshold from above, and two from below. The two highest curves are fully repulsive and can support no resonances. The lowest curve, which has a designation of $(2,0)^+$ in terms of the $(K,T)^A$ quantum numbers, see Lin [25], supports an infinite series of resonances, of which four are included in Table I with identification $N(K,T)^A_n$; n is the principal quantum number of the outer electron. If a single-channel approximation is valid and if the resonances are dominated by the asymptotic dipole potential, then the positions $\epsilon_{N,n}$ measured from the H(N) threshold and the widths $\Gamma_{N,n}$ of succes-

TABLE I. Energies E_r and widths Γ (in a.u.) of resonance states of $H^-(^3P^o)$ near the $H(N=3)$ threshold. $1.65[-3] = 1.65\times10^{-3}$.

	Present		Complex coordinate[a]		*R* matrix[b]	
Classification	$-E_r$	Γ	$-E_r$	Γ	$-E_r$	Γ
$3(2,0)^+_3$ (Feshbach)	0.06791	1.65[−3]	0.06791	1.71[−3]	0.06792	1.64[−3]
$3(2,0)^+_4$ (Feshbach)	0.05743	3.04[−4]	0.05742	3.03[−4]	0.05742	3.09[−4]
$3(1,1)^-_4$ (Feshbach)	0.05640	4.15[−6]	0.05638	4.00[−6]	0.05638	4.4 [−6]
$3(2,0)^+_5$ (Feshbach)	0.05592	6.42[−5]	0.05591	5.65[−5]	0.05591	6.36[−5]
$3(2,0)^+_6$ (Feshbach)	0.05563	1.33[−5]	0.05562	1.20[−5]		
$3(0,0)^+_3$ (shape)	0.05478	8.92[−4]	0.05475[c]	8.5 [−4][c]	0.05530	6.0 [−6]

[a]Reference [13].
[b]Reference [19].
[c]Reference [12].

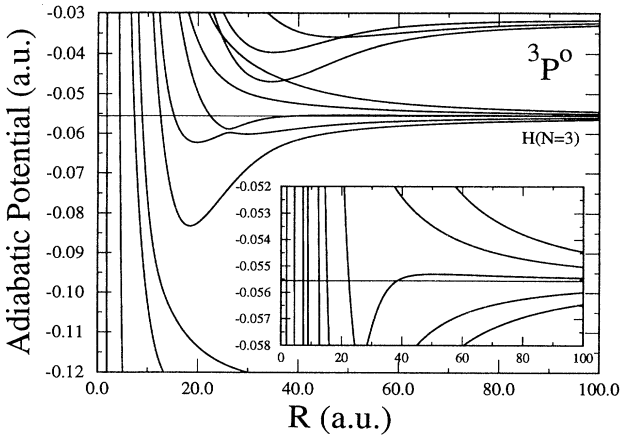

FIG. 3. Adiabatic potential curves of $H^-(^3P^o)$ as functions of hyperradius R. The thin horizontal line indicates the $H(N=3)$ threshold. The inset is a magnification of a part near this threshold.

sive resonances are related by

$$\frac{\epsilon_{N,n}}{\epsilon_{N,n+1}} = \frac{\Gamma_{N,n}}{\Gamma_{N,n+1}} = \exp\{2\pi(-a_j - \tfrac{1}{4})^{-1/2}\},$$

where a_j is the strength of the dipole potential in the jth asymptotic uncoupled equation [19]. The ratio expected from the dipole potential is 5.16 for the $(2,0)^+$ channel, the ratios of the energy positions of the successive $(2,0)^+$ resonances in Table I are 5.47, 4.75, and 4.82, and the ratios of the widths are 5.36, 4.73, and 4.83, respectively.

Figure 3 shows an avoided crossing between the second and the third curves of the $N=3$ manifold. The $(K,T)^A$ character is preserved as the avoided crossing is crossed diabatically. Thus the second curve at small R, having a $(0,0)^+$ character, may be connected diabatically into the third curve at large R having the same character. This curve crosses the $H(N=3)$ threshold near $R=36$ and has

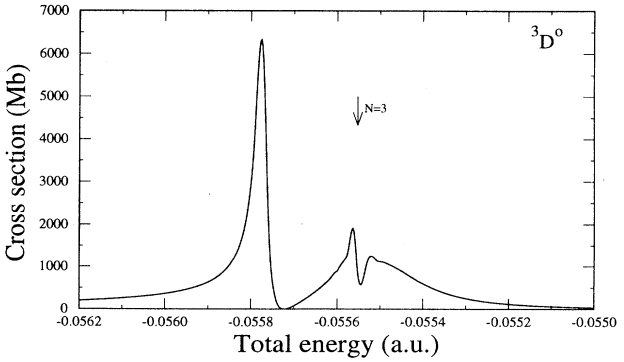

FIG. 4. Cross section for photodetachment from the $H^-(2p^2\,^3P^e)$ state to the final state $H(2p)+\epsilon d$ $(^3D^o)$ in the energy region close to the $H(N=3)$ threshold indicated by the downward arrow.

TABLE II. Energies E_r and widths Γ (in a.u.) of resonance states of $H^-(^3D^o)$ near the $H(N=3)$ threshold. $3.15[-5] = 3.15\times10^{-5}$.

	Present		Complex coordinate (Ref. [13])	
Classification	$-E_r$	Γ	$-E_r$	Γ
$3(1,1)_4^-$ (Feshbach)	0.05578	3.15[−5]	0.05577	3.8[−5]
$3(0,2)_3^+$ (shape)	0.05555	2.46[−4]	0.05550	2.8[−4]

a potential barrier, which supports the shape resonance as seen in Fig. 2. The third curve at small R connects diabatically to the second curve at large R. This diabatic potential is labeled as the $(1,1)^-$ curve, and supports the third Feshbach resonance listed in Table I. It was demonstrated and explained before [3,11] that many $A=-$ resonances, weakly populated in photoabsorption spectra from tightly bound states, are greatly enhanced in photoabsorption from excited states. Here is still another example where the initial state is an extremely weakly bound state.

C. $^3D^o$ resonances near the $H(N=3)$ threshold

Photoabsorption from the $^3P^e$ state also populates $^3D^o$ final states. There is only one final channel in Eq. (3) having this symmetry, and this channel produces $H(2p)$. The contribution to the $2p$ partial cross section from this channel is shown in Fig. 4, where two Feshbach resonances and one shape resonance are clearly seen. The positions and widths of the first Feshbach resonance and the shape resonance are given in Table II and are compared with the calculations by Ho [13]. The agreement is satisfactory.

To analyze the origin of these resonances, we show adiabatic hyperspherical potential curves of $^3D^o$ symmetry in Fig. 5. The avoided crossing between the first

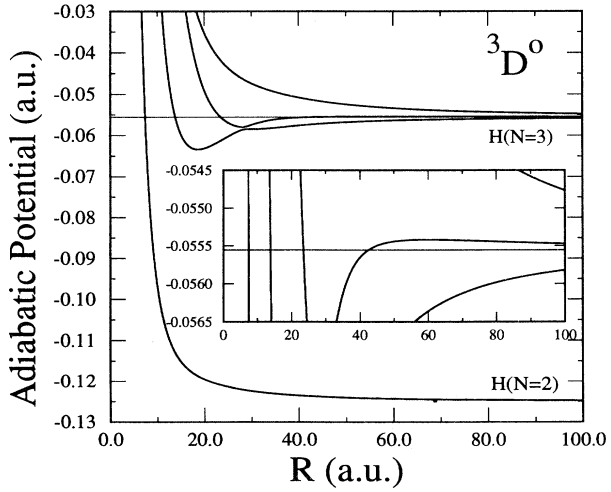

FIG. 5. Adiabatic potential curves of $H^-(^3D^o)$ as functions of hyperradius R. The thin horizontal line indicates the $H(N=3)$ threshold. The inset is a magnification of a part near this threshold.

two $N=3$ curves may be treated as a diabatic crossing, and a single-channel approximation may be made, as in Sec. III B. The diabatic curve that supports the shape resonance is the $(0,2)^+$ curve, which has an attractive well at small R, crosses the H($N=3$) threshold near $R=42$, and has a repulsive barrier at large R. The two Feshbach resonances are supported by the $(1,1)^-$ potential, which is repulsive at small R but is an attractive dipole potential at large R. These $(1,1)^-$ resonances exemplify the enhanced $A=-$ resonances in photoabsorption by weakly bound states, just like the $^3P^o$ $(1,1)^-$ resonances discussed in Sec. III B.

IV. SUMMARY

We have studied the photodetachment spectrum of H^- from the weakly bound $2p^2\,^3P^e$ state using the hyperspherical close-coupling method. We have shown that the partial cross sections for leaving the hydrogen atom in the $2s$ and $2p$ excited states are in good agreement with the close-coupling calculations of Jacobs *et al.* [14] in a low-energy region. At even lower energies than those covered by Jacobs *et al.*, the photodetachment cross sections drop rapidly toward the H($N=2$) threshold in agreement with the results of Du *et al.* [15], who carried out semiempirical adiabatic hyperspherical-coordinate calculations.

We have also extended our calculations to higher energies to analyze resonances near the H($N=3$) threshold. We have found two series of Feshbach resonances of $^3P^o$ symmetry, one series of Feshbach resonances of $^3D^o$ symmetry, and one shape resonance of each of these symmetries. The existence of shape resonances just above high-N excitation thresholds appear to be quite common in H^-. Using diabatic hyperspherical potential curves, we have assigned the correlation quantum numbers K, T, and A to these Feshbach and shape resonances. Some $A=-$ resonances are clearly seen in the photodetachment spectrum, which is characteristic of photoabsorption by weakly bound states [3,11]. The calculated resonance positions and widths are in good agreement with the variational results obtained by Ho and Bhatia [12,13] using the complex-coordinate rotation method.

ACKNOWLEDGMENTS

This work was supported in part by the U.S. Department of Energy, Office of Energy Research, Office of Basic Energy Sciences, Division of Chemical Sciences. One of the authors (J.-Z. T.) was supported by the Special Researchers' Basic Science Program of RIKEN.

[1] J.-Z. Tang, Y. Wakabayashi, M. Matsuzawa, S. Watanabe, and I. Shimamura, Phys. Rev. A **49**, 1021 (1994).
[2] M. Halka, H. C. Bryant, C. Johnstone, B. Marchini, W. Miller, A. H. Mohagheghi, C. Y. Tang, K. B. Butterfield, D. A. Clark, S. Cohen, J. B. Donahue, P. A. M. Gram, R. W. Hamm, A. Hsu, D. W. MacArthur, E. P. MacKerrow, C. R. Quick, J. Tiee, and K. Rózsa, Phys. Rev. A **46**, 6942 (1992).
[3] J.-Z. Tang and I. Shimamura, Phys. Rev. A **51**, R1738 (1995).
[4] P. G. Harris, H. C. Bryant, A. H. Mohagheghi, R. A. Reeder, H. Sharifian, C. Y. Tang, H. Tootoonchi, J. B. Donahue, C. R. Quick, D. C. Rislove, W. W. Smith, and J. E. Stewart, Phys. Rev. Lett. **65**, 309 (1990).
[5] J.-Z. Tang, S. Watanabe, and M. Matsuzawa, Phys. Rev. A **46**, 2437 (1992).
[6] J.-Z. Tang, S. Watanabe, M. Matsuzawa, and C. D. Lin, Phys. Rev. Lett. **69**, 1633 (1992).
[7] J.-Z. Tang, S. Watanabe, and M. Matsuzawa, Phys. Rev. A **48**, 841 (1993).
[8] B. Zhou, C. D. Lin, J.-Z. Tang, S. Watanabe, and M. Matsuzawa, J. Phys. B **26**, 2555 (1993).
[9] B. Zhou, C. D. Lin, J.-Z. Tang, S. Watanabe, and M. Matsuzawa, J. Phys. B **26**, L337 (1993).
[10] B. Zhou and C. D. Lin, Phys. Rev. A **49**, 1057 (1994).
[11] J.-Z. Tang and I. Shimamura, Phys. Rev. A **50**, 1321 (1994).
[12] Y. K. Ho and A. K. Bhatia, Phys. Rev. A **48**, 3720 (1993).
[13] Y. K. Ho (private communication).
[14] V. L. Jacobs, A. K. Bhatia, and A. Temkin, Astrophys. J. **202**, 1278 (1980).
[15] N.-Y. Du, A. F. Starace, and M.-Q. Bao, Phys. Rev. A **50**, 4365 (1994).
[16] A. F. Starace (private communication).
[17] M. J. Seaton, Proc. Phys. Soc. London **77**, 174 (1961).
[18] M. Gailitis and R. Damburg, Proc. Phys. Soc. London **82**, 192 (1963).
[19] A. Pathak, A. E. Kingston, and K. A. Berrington, J. Phys. B **21**, 2939 (1988).
[20] C. H. Greene, U. Fano, and G. Strinati, Phys. Rev. A **19**, 1485 (1979).
[21] G. W. F. Drake, Phys. Rev. Lett. **24**, 126 (1970).
[22] J.-Z. Tang, S. Watanabe, and M. Matsuzawa, Phys. Rev. A **46**, 3758 (1992).
[23] C. H. Greene and A. R. P. Rau, Phys. Rev. A **32**, 1352 (1985).
[24] U. Fano, Phys. Rev. **124**, 1866 (1961).
[25] C. D. Lin, Phys. Rev. A **29**, 1019 (1984); Adv. At. Mol. Phys. **22**, 77 (1986).